Towards long-multitemporal change detection using SVI differencing by integrated DWT-ISOCLUS: A model for forest temporal dynamics mapping

Article *in* International Journal of Digital Earth · March 2011

DOI: 10.1080/17538941003610920 · Source: DBLP

2 authors:

Yashon Ouma
Moi University

Ryutaro Tateishi
Chiba University

International Journal of Digital Earth

ISSN: 1753-8947 (Print) 1753-8955 (Online) Journal homepage: https://www.tandfonline.com/loi/tjde20

Towards long-multitemporal change detection using SVI differencing by integrated DWT–ISOCLUS: a model for forest temporal dynamics mapping

Yashon O. Ouma & Ryutaro Tateishi

International Journal of Digital Earth,
Vol. 4, No. 2, March 2011, 108–132

Taylor & Francis
Taylor & Francis Group

Towards long-multitemporal change detection using SVI differencing by integrated DWT–ISOCLUS: a model for forest temporal dynamics mapping

Yashon O. Ouma[a]* and Ryutaro Tateishi[b]

[a]*Tateishi Laboratory, Centre for Environmental Remote Sensing (CEReS), Graduate School of Science and Technology, Chiba University, 1-33 Yayoi-cho, Inage-ku, Chiba 263-8522, Japan;* [b]*Tateishi Laboratory, Centre for Environmental Remote Sensing (CEReS), Chiba University, 1-33 Yayoi-cho, Inage-ku, Chiba 263-8522, Japan*

(Received 3 November 2009; final version received 10 January 2010)

Characterisation and mapping of land cover/land use within forest areas over long-multitemporal intervals is a complex task. This complexity is mainly due to the location and extent of such areas and, as a consequence, to the lack of full continuous cloud-free coverage of those large regions by one single remote sensing instrument. In order to provide improved long-multitemporal forest change detection using Landsat MSS and ETM + in part of Mt. Kenya rainforest, and to develop a model for forest change monitoring, wavelet transforms analysis was tested against the ISOCLUS algorithm for the derivation of changes in natural forest cover, as determined using four simple ratio-based Vegetation Indices: Simple Ratio (SR), Normalised Difference Vegetation Index (NDVI), Renormalised Difference Vegetation Index (RDVI) and modified simple ratio (MSR). Based on statistical and empirical accuracy assessments, RDVI presented the optimal index for the case study. The overall accuracy statistic of the wavelet derived change/no-change was used to rank the performances of the indices as: RDVI (91.68%), MSR (82.55%), NDVI (79.73%) and SR (65.34%). The integrated discrete wavelet transform–ISOCLUS (DWT–ISOCLUS) result was 42.65% higher than the independent ISOCLUS approach in mapping the change/no-change information. The methodology suggested in this study presents a cost-effective and practical method to detect land-cover changes in support of decision-making for updating forest databases, and for long-term monitoring of vegetation changes from multisensor imagery. The current research contributes to *Digital Earth* with regards to geo-data acquisition, data mining and representation of one forest systems.

Keywords: digital earth; long-multitemporal forest change detection; Spectral Vegetation Index Differencing (SVID); ISOCLUS; discrete wavelet transform (DWT); integrated DWT–ISOCLUS

1. Introduction

Despite the efforts by governments and conservation organisations, tropical deforestation – mainly conversion of forest to agricultural land, continues to proceed at an alarmingly high rate, and is estimated at 9.2 million hectares per year from remote sensing survey (FAO 2006). Conservation of these tropical forests is very

*Corresponding author. Email: yashon@graduate.chiba-u.jp

ISSN 1753-8947 print/ISSN 1753-8955 online

DOI: 10.1080/17538941003610920
http://www.informaworld.com

crucial for species diversity, climate stability and carbon cycle. Forest monitoring, in form of change detection, is thus required to provide timely and reliable information on forests condition, composition, and extent for making good decisions in forest management and planning at a large scale.

Land use and land cover change (LUCC), in general, is increasingly recognised as an important driver of environmental change on all spatial and temporal scales. LUCC contributes significantly to earth atmosphere interactions, forest fragmentation and biodiversity loss. It has become one of the major issues for environmental change monitoring and natural resource management. LUCC and its impacts on terrestrial ecosystems including forestry, agriculture and biodiversity have been identified as high priority issues in global, national and regional levels. Land use and land cover, as the basic spatial element of landscape, plays an important role in the study of landscape ecology. Analysis of the relationship between landscape spatial patterns and functions is based on the accurate and timely information of land use and land cover.

The Kenyan landscape, as in many developing countries, has undergone significant forest changes. The extent of native forests in Kenya has steadily decreased since independence, i.e. from 1964 to date. The establishment of human settlements, logging and a range of other factors have all reduced forest cover, however it is land clearing for agriculture that has been the most significant process by far, and is a process that continues today. This land cover/land use dynamics has greatly affected the main watersheds that also act as the key water towers in Kenya such as: Mt. Kenya, Mau Ranges, and the Aberdare ranges.

At the sub-regional level, wide-scale land clearing, subsequent abandonment of small-scale agricultural areas and several bush fires has resulted in severe landscape disturbance in the Mt. Kenya ranges. Land use and land cover have undergone further significant changes with the establishment of large-scale plantations in the area over the last five decades. Consequently, all areas bordering the cool temperate rainforest of the Mt. Kenya region are a mosaic of different land use histories formatted by both natural and human disturbances. The different land use patterns have different influences on imbedded remnant patches of cool temperate rainforest mainly through edge effects, i.e. regions adjacent to the forest.

However, details of LUCC and its influence on the rainforest in this area are yet to be assembled and interpreted. This study aims to model the long-term LUCCs, from 1976 to 2000, in the Mt. Kenya ranges by integrating remote sensing (Landsat MSS and ETM+) and historical aerial photography, to aid in the provision of quantitative analysis of LUCC information in the area.

The characterisation and mapping of land cover/land use of forest areas over long-multitemporal intervals is a complex task. This complexity is mainly due to the extent of such areas and, as a consequence, to the lack of full continuous cloud-free coverage of those large regions by one single remote sensing instrument. Further, determination of large natural forest disturbances is time-consuming, difficult and expensive through conventional field surveys or by means of aerial photo interpretation.

Digital multitemporal satellite data with their ability to cover large areas at relatively low costs and revisit frequency has created a high potential for natural forest change detection. Different techniques have been reported for detecting forestland cover change detection from multitemporal remote sensing data sets. In literature, more than 50 Vegetation Indices (VIs) (Bannari *et al.* 1995) have been developed for different applications. Normalised difference vegetation index (NDVI) differencing is the commonly used technique for vegetation dynamics modelling (Lyon *et al.* 1998, Fung and Siu 2000, Young and Wang 2001, North 2002). While NDVI is the most popular index, it has also undergone several transformations to minimise soil and atmospheric effects, resulting in NDVI-related indices, which are also functions of the simple ratio (SR) index. The SR indices arguably have higher correlations with the field data.

The aim of this study is to investigate on the applicability of SR-based Spectral Vegetation Indices (SVIs) for unsupervised forest disturbances detection. In this study, SVIs that are based on SR, and developed to minimise the soil and atmospheric effects are used for forest disturbance detection. The four SVIs tested in this study include: (i) SR; (ii) NDVI; (iii) Renormalised Difference Vegetation Index (RDVI) (Roujean and Breon 1995); and the (iv) modified simple ratio (MSR) (Chen 1996). Scene-based comparative studies by Kalácska *et al.* (2004) showed that MSR performed better than other SVIs like SR, NDVI, Non-Linear Index (NLI), Soil-Adjusted Vegetation Index-2 (SAVI2) and Infrared Index (IRI). Such conclusions cannot however be generalised as they may not necessarily hold for all scenes under investigation. Similarly, Coppin and Bauer (1996) reported that image differencing and linear transformations generally performed better than other methods (i.e. post-classification comparison methods (delta comparison); mono-temporal change delineation; multi-dimensional temporal feature space analysis; composite analysis; change vector analysis (CVA)) in forest mapping and change detection. The advantage of image differencing and linear transformation is in the ability of these algorithms to utilise suitable image bands with inherent thresholds through indices for the identification of the stable sub-space and emphasis of the multitemporal data.

1.1 Objectives of the current study

This study proposes to use the combination of image differencing and linear transformations, based on the comparison of the SR-derived VIs. The specific objectives are to determine:

1) the optimal SVI for deriving forest disturbances in part of Mt. Kenya over the 25-year span from natural forest to other land use using Landsat MSS and ETM+;
2) whether the scale-dependent wavelet transform analysis can reveal the localised relationships between forest cover changes, in comparison with the scale-invariant spectral clustering approaches, i.e. ISOCLUS, for change information extraction from the SVI difference image.

The proposed approach is a deviation from the conventional use of semi-automatic trial-and-error thresholding techniques. The main assumption made in this study is to ignore the slight differences in the sensor wavelengths, due to the inherent design specifications of the Landsat ETM+ and Landsat MSS sensor systems (Carvalho *et al.* 2001).

The relevance of this paper to *Digital Earth* lies on the benefit in the digital geo-data acquisition, data mining and representation of one of the key components of the earth i.e. forest dynamics or space–time digital representation and analysis. Such data goes along way in informing the public sector, private sector and decision makers in the collective conservation and management of the earth. The model presented in this paper can be extended to the national, trans-boundary and global visualisation of the forest dynamics, much more accurately, via more intelligent digital image descriptors.

1.2 Vegetation dynamics and multiscale representation: the study motivation

Reflectance of vegetation is a complex modelling exercise. Leaf reflectance is influenced by the concentration of leaf biochemicals, water content and leaf structure. All these constituents are variable in time and space. Temporal change is induced by climate, catastrophic events (floods, fire, drought, disease) and anthropogenic activities. The expression of temporal change is elicited by phenology (annual cyclic process) and the diurnal cycle of the opening and closing of stomata in the leaf. The stomata regulate the exchange of moisture, CO_2 and O_2. Spatial differences in leaf characteristics result from species differences (needle leaf and broadleaf), but also with the same species, spatial stratification of leaves has a strong impact on canopy reflectance. The cell walls within the leaf cause multiple scattering in many directions, depending on the angle between incident light and the orientation of the cell walls. On the other hand, the waxy layer covering the leaf epidermis (cuticle) results in a strong specular component. The foregoing argument complicates change detection in forest environments.

The complexity of vegetation modelling and mapping requires integrated-complimentary approaches. The motivation to this proposed approach is that in order to improve the accuracy of the change maps, a multiscale strategy can be adopted, in which transformed images at different scales are jointly used. The images at the finest scales are likely to highlight many geometrical details, but also to be more affected by noise. Data at coarser scales exhibit less precise details, but a stronger immunity to noise. A multiscale approach, exploiting coarser scales to globally identify changed areas and finer scales to improve the detection of details, may represent an effective choice.

The rest of this paper is organised as follows. Section 2 is on the study area, data and radiometric normalisation of the data sets. Section 3 presents the proposed methodology on forest change detection using SVIs, followed by SVI image differencing (SVID), and then feature extraction from the SVID images using wavelets analysis and ISOCLUS. Sections 4 and 5, respectively, present the study results and discussions. The study summary and conclusions are drawn in Section 6.

2. Materials

2.1 Study area and data

The study area is part of Mt. Kenya, located centrally at approximately 0° 09′ S and 37° 18′ E (Figure 1a(i)). Mt. Kenya is one of the significant natural ecological units

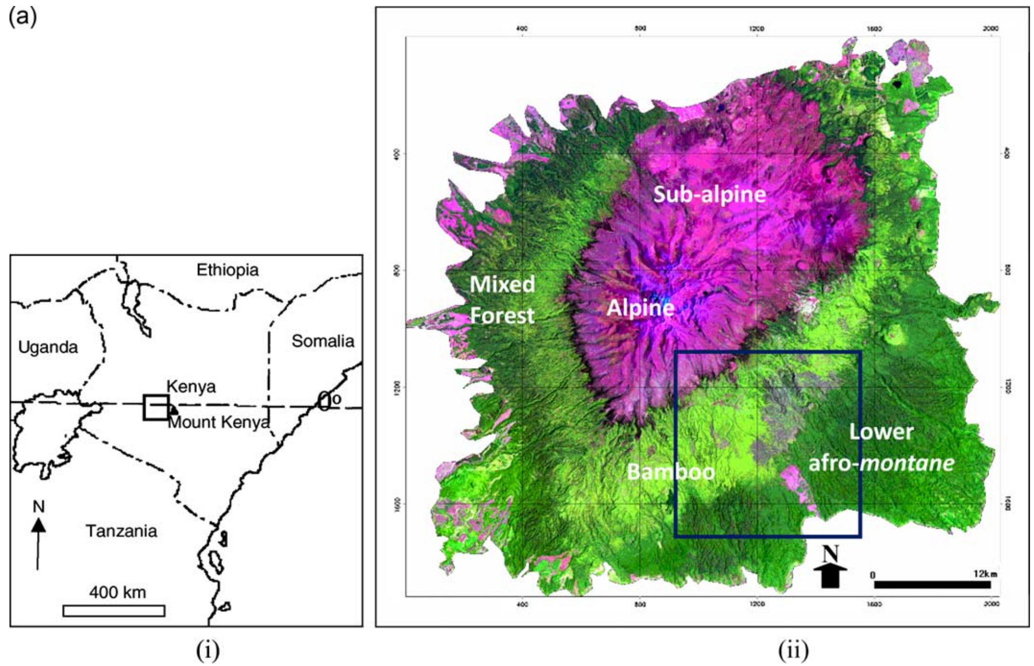

Figure 1a. (i) Map of Kenya and the location of Mt. Kenya. (ii) Landsat ETM+bands 543 of Mt. Kenya. The rectangular outline shows the delineated study area, which is shown in Figure 1b.

in Kenya, enclosing a total area of about 3132.56 km^2. The top sub-alpine and alpine belts; mixed forests, bamboo in the middle and afromontane forests at the bottom, characterise the mountain. Due to the wide range of altitude that spans the indigenous forest zone (from altitude 1200 to 3400 m), and the major climatic differences between the slopes, the forest vegetation of Mt. Kenya is characterised by a high diversity of forest types and various vegetation zones can be distinguished on Mt. Kenya (Figure 1a(ii)).

For purposes of this study, a selected section of Mt. Kenya (enclosed rectangular region in (Figure 1a(ii)) was chosen. Figure 1b shows the selected study area of bands 431 false colour composite (FCC) corresponding to Landsat MSS and ETM+ images. The data sets were taken in the same time epoch (during the semi-dry season of January of the corresponding years). This time was taken following an in-depth analysis of the two main seasons (rainy and dry), to ensure no erratic differences in the climatic conditions that may influence the phenological conditions, for accurate long-multitemporal change detection. While in 1976 most of the forestland was undisturbed, by 2000 most of the forest had experienced significant disturbances resulting from natural- and human-based activities.

2.2 Data correction

The two Landsat data sets were geometrically rectified to the Universal Transverse Mercator (UTM) map projection system-Zone 37 East. Aerial photographs and a 1:50,000 topographical map of 1997 were used to derive the ground control points (GCPs) for the geometric correction.

The Landsat ETM + was first geometrically referenced to an accuracy of less than half a pixel (<15 m). Nearest-neighbour resampling method was used to resample the ETM+ to 60 m $\times$ 60 m pixel size in order to allow for pixel–pixel comparison with MSS (of spatial resolution of 60 m $\times$ 60 m), and to avoid altering the original pixel values of the MSS image. It is notable that the degrading of the spatial resolution from 30 to 60 m did not degrade the scene features an the point locational accuracy, since the landscape features being dealt with in this study scene were generally larger than 60 m. The choice of nearest-neighbour resampling was preferred in order to minimise on the textural properties, especially for not very large textured landscapes, since wavelet transformation is used to describe textural properties at different resolutions. Image-to-image registration was then used to geometrically rectify the MSS to ETM+ with an RMS error of approximately 15 m.

To normalise the test data sets for accurate change detection, temporally pseudo-invariant features (PIF), determined on the ground and image, were used as reference for digital number (DN) correction. From empirical image investigations, the Landsat MSS data was noisier as a result of the stripping effect (Figure 1b(i)). The noise was particularly prominent at the low digital values (the darker image components). Low and high image DN values corresponding to features of dark and bright pixels, respectively, were used. The PIF correction was implemented based on the empirical line (EL) approach (PIF-EL) (Figure 2).

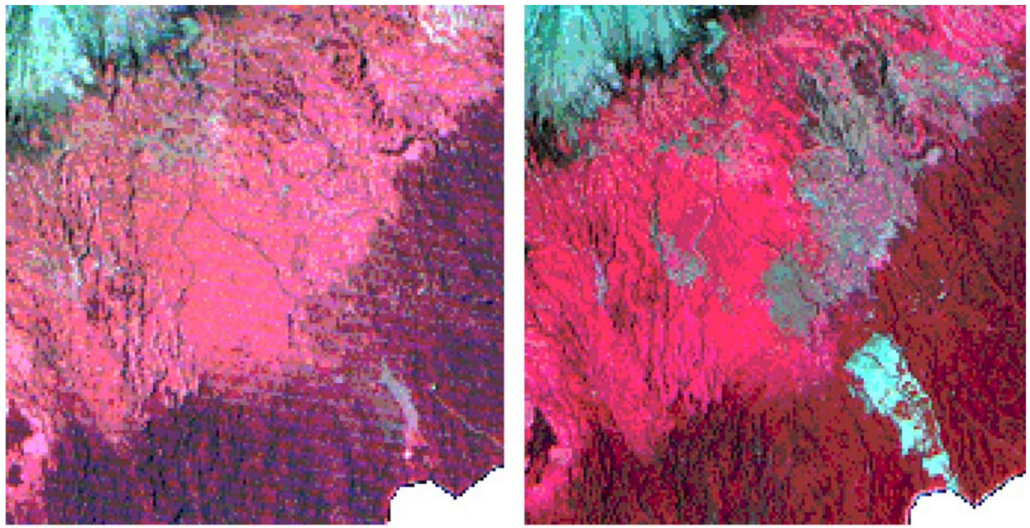

(b) (i) (ii)

Figure 1b. False colour composite of bands 431 of the test site for: (i) Landsat MSS (1976) and (ii) Landsat ETM+(2000).

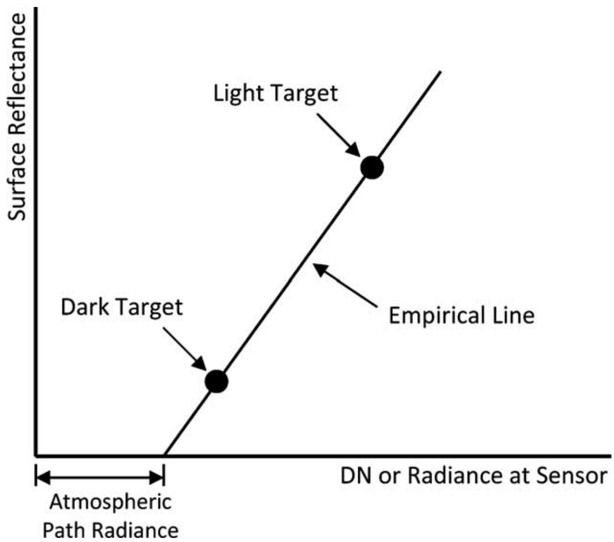

Figure 2. The concept of empirical line (EL) using two targets of contrasting albedo for radiometric normalisation.

The EL method is an atmospheric correction technique that provides an alternative to radiative transfer modelling approaches. It offers a relatively simple means of surface reflectance calibration, providing that a series of invariant-in-time calibration target measurements are available. This technique has been applied with variable success to both airborne data and coarser spatial resolution satellite sensor data (Karpouzli and Malthus 2003). It assumes that a linear relationship exists between image DNs and ground-measured reflectance for surfaces with a range of contrasting albedo. This linear relationship is used to calculate gains and offsets that convert DNs to reflectance factors (Clark *et al.* 2002). Researchers (e.g. Clark *et al.* 1997, Goetz *et al.* 1998) have used combinations of radiative modelling approaches and empirical approaches for the derivations of surface reflectances from imaging data.

The simplest approach to EL calibration is to use one target and assume that a dark ground surface will produce a DN of zero. Using two targets of contrasting albedo, or the two-target approach, allow the calibration to account for atmospheric scattering. Generally, a linear relationship between ground spectral measurements and image DNs is realised with more points, which is a factor of the size of the scene. The ground target surfaces used were: (i) homogeneous; and (ii) comprised of pixels of contrasting albedo. The calculated reflectance factor values were typically considered valid only between the bright and dark target extremes and extrapolation outside this range was avoided. The same ground surfaces were also used in the change detection accuracy assessment.

Historical aerial photographs, ground reconnaissance at the forest edge, 1:50,000 topographical map and the FCC images were compared and used for ground-reference. A total of 30 homogenous evaluation regions were selected as reference, partly for the PIF-EL radiometric normalisation and partly for the change detection accuracy assessment and validation.

3. Theoretical background and experimental procedure

The fundamental theory behind the utility of SVI is that a leaf and thus the canopy radiative transfer model should provide leaf reflectance and transmittance from leaf biochemical content (chlorophyll, water content and dry matter) and structural (textural and spatial) parameters. However, with remote sensing and the use of airborne or spaceborne spectrometers, it is canopy reflectance which is measured, not leaf reflectance. In that respect, the up-scaling from a single leaf to canopy is not a trivial task. The transition from the leaf to the canopy level introduces effects due to, e.g. variable solar illumination intensity and angles of observation, atmospheric conditions, vegetation canopy architecture and under-storey. Thus the strategy in this study is to model the biochemical contents and the structural parameters, through an integrated SVI and wavelet transform approach.

3.1 Forest change detection using Spectral Vegetation Index Differencing (SVID)

According to Chen (1996), the SR index, and its associated indices (NDVI, RDVI and MSR) are better correlated to the field data than do the rest of the indices that cannot be expressed as a function of SR. Many unwanted noises cause simultaneous increases or decreases in red and NIR reflectance in approximately the same proportion, and therefore they can be greatly reduced by taking the SR. Indices such as NLI, SAVI-2, and Global Environmental Monitoring Index (GEMI), that employ mathematical operations other than ratioing, amplify the noise. Indices such as weighted difference vegetation index (WDVI) and perpendicular vegetation index (PVI) based on the absolute difference between the reflectance retain the noises. The major draw back of SAVI and SAVI-1 is the reduction of their sensitivity to surface parameters of interest because of the use of the parameter (L) in the denominator. L dampens the background effect at the expense of the sensitivity (Chen 1996).

From the foregoing exposition, the following indices, represented by Equations (1)–(4), were compared for the case study:

$$\mathrm{SR} = \rho_{\mathrm{NIR}}/\ \rho_R \tag{1}$$

$$\mathrm{NDVI} = (\rho_{\mathrm{NIR}} - \rho_R)/(\rho_{\mathrm{NIR}} + \rho_R) \tag{2}$$

$$\mathrm{RDVI} = ((\rho_{\mathrm{NIR}} - \rho_R)/(\rho_{\mathrm{NIR}} + \rho_R))^{1/2} \tag{3}$$

$$\mathrm{MSR} = \left(\frac{\rho_{\mathrm{NIR}}}{\rho_{\mathrm{R}}} - 1\right)\Big/\left(\frac{\rho_{\mathrm{NIR}}}{\rho_R} + 1\right)^{1/2} \tag{4}$$

In the above equations, ρ_{NIR} and ρ_R refer to the recorded ground reflectance in NIR and R bands, respectively. Equations (2) and (4) can be re-written in terms of Equation (1) as: $\mathrm{NDVI} = (\mathrm{SR} - 1/\mathrm{SR} + 1)$ and $\mathrm{MSR} = (\mathrm{SR} - 1/(\mathrm{SR} + 1)^{1/2})$, respectively.

From the corrected MSS and ETM+ data sets, the corresponding image differences (SVID) are derived for multitemporal change detection. However, the results of such SVID imagery do not automatically decipher the desired change/no-change features or classes. In common practice, trial-and-error-based thresholding procedures are employed to map the change/no-change information. More advanced parametric Bayesian approaches can also be used. However, in productive applications, automated temporal feature dynamics needs to be adopted especially for the long-multitemporal scenes, especially where training data is unattainable exactly at the image acquisition time. Thus, the strategy in this study is to model the biochemical contents using the SV indices and the structural parameters using the wavelet transform, in sequential processing fashion.

Arguing that a clustering algorithm is suitable for mapping the change/no-change information, the proposed technique (Figure 3) explores the theoretical proposition of capturing change via SVID followed by a multiscale feature extraction using discrete wavelet transform (DWT) and subsequently class identification using ISOCLUS unsupervised algorithm, hence the DWT–ISOCLUS approach. The proposed approach uses the ability of unsupervised classifier (ISOCLUS (PCI 1999)), in comparison with the integrated scale-based information extraction (DWT–ISOCLUS), to automatically and finally segment the different classes represented in the SVID image.

While the SVID image provides the spectrally segmented information, the DWT extracts the textural image feature components. The advantage of using DWT is its ability to capture and separate the image local features at different informative scales.

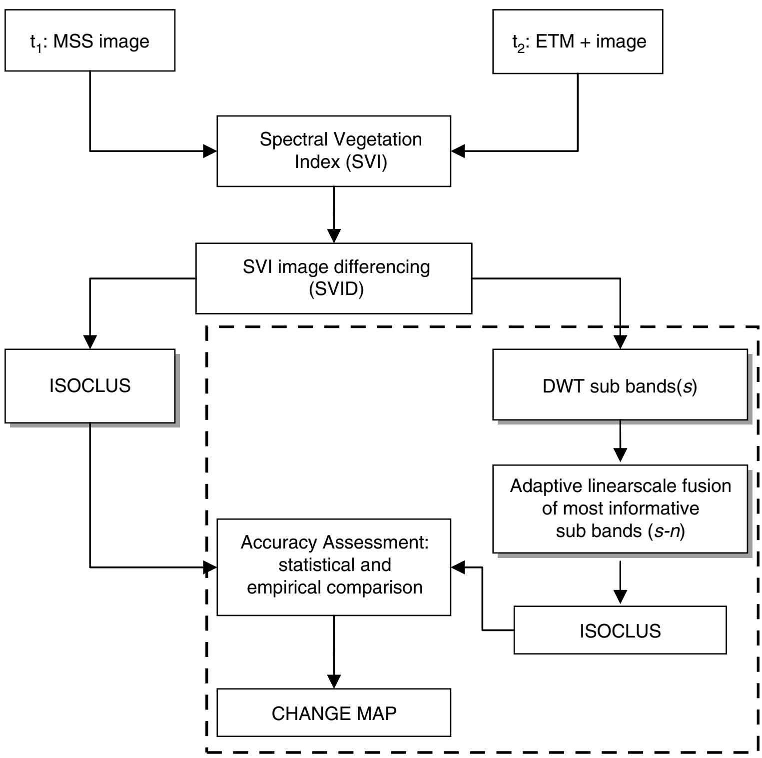

Figure 3. Block scheme of the proposed change-detection approach. t_1 and t_2 are the two time epochs corresponding to MSS and ETM+, respectively, and DWT is the discrete wavelet transform. (The dotted outline is the DWT–ISOCLUS algorithm).

These informative scales can then be linearly fused/combined (Figure 3), to take advantage of the finer and coarser scales.

3.2 Discrete wavelet transform (DWT) representation and image feature analysis

Briefly, a wavelet decomposition of any given signal (1-D or 2-D) is the process which provides a complete representation of the signal according to a well-chosen division of the time-frequency (1-D) or space-frequency (2-D) plane. Through iterative filtering by low and high-pass filters, it provides information about low and high-frequencies of the signal at successive spatial scales (Yu and Ekström 2003, Memarsadeghi *et al.* 2006).

An s-scale multiresolution decomposition of the difference image D (s being a predefined number of scales) is obtained by applying a dyadic DWT. D is decomposed in terms of a low-pass transformed image and of three transformed images conveying high-pass information about fine-scale details along the horizontal image axis, the vertical axis, or both axes. Then, the procedure is recursively applied S times to the low-pass component. As s increases in [1, s], coarser-scale approximations of D are obtained, while the finest scale is D itself. More precisely, detail components allows appreciating spatial details that are (2^s)-times coarser than the original image $D_0(s = 1,2, \ldots S)$. See Mallat (1989) and Daubechies (1991) for general theoretical background on wavelet transforms.

Multiresolution wavelet transforms, that are largely used for data compression and browsing, are utilised in this study:

1) As a way to bring multiple types of data to the same spatial resolution without losing significant information and without blurring the higher resolution data. Multi-resolution wavelet decomposition preserves most of all important features of the original data even at a lower resolution, especially global scale features. We argue that scene changes are related to the scale, different changes can be obtained at different scales for the same images, and the basic strategy is therefore to build up a hierarchical network of change maps which represent the change information at different scales simultaneously. Once the changes at each scale have been detected, it is possible to derive more reliable change map according to a proper multiscale fusion strategy.
2) For feature extraction purposes from the SVID image. Multiresolution wavelet decomposition separates high and low-frequency components which are then recomposed differently in the selective scale-driven fusion phase.

In this study, the Mexican hat wavelet, with the wavelet function defined by the equation $\Psi(x, y) = (1 - x^2 - y^2)^* e^{-(x^2+y^2)/2}$, was selected due to its shape and irregular edges approximation abilities that approximates the forest canopies and irregularly shaped farmlands and logged patches. The 2-D Mexican hat wavelet basis function was successively convolved, over a range of five-dilation scales. However, the significance of these levels must be quantified to retain or discard a level or its sub-band for further processing, in this case fusion of most informative sub-bands. Only the detail sub-bands were used for this study, since the approximation image does not isolate any specific-scene features and the associated structural properties.

One major advantage afforded by wavelets is the ability to perform local analysis. That is to analyse a sub-image area of a larger image. Wavelet analysis is capable of revealing aspects of data that other signal analysis techniques usually miss, like trends, breakdown points, discontinuities in higher derivatives and signal component similarities (Yu and Ekström 2003). Further, the DWT approach results in minimal redundancy in the features that are detected at specific sub-bands and scales. This makes the multiscale fusion viable with very minimal feature misrepresentation.

3.2.1 Discrete wavelet transform (DWT) informative level(s) selection strategy

The wavelet-subband energy content determination, Equation (5), was used to aid in the selection of the significant sub-bands to be combined/linearly fused for further processing.

$$E_j^i = \frac{1}{MN} \sum_{m=1}^{M} \sum_{n=1}^{N} (f_j^i(m,n))^2 \tag{5}$$

where: $M,\ N =$ the size of given scope; $f_j^i(m,n) =$ the element of sub-band from wavelet transform; $j =$ the direction of the wavelet transform, and $i =$ the level of wavelet transform. E_j^i is the wavelet energy signature reflecting the distribution of energy along the frequency axis over scale and orientation, and varies according to the information contained in a sub-band and its magnitude can be used to judge the relevance of the level and its sub-bands, through comparison of the energy of the successive levels.

Given that the image (f) can be represented in terms of the low-frequency (A) and the high-frequency imagery sub-bands (horizontal (H); vertical (V) and diagonal (D)) as: ($f = A_l + \Sigma_{i=1}^{l}(H_i + \mathrm{V}_i + \mathrm{D}_i)$) after l-level decomposition, then it is possible to combine or linearly fuse the most informative high-frequency sub-bands as proposed in Figure 3.

3.3 ISOCLUS for change information extraction

ISOCLUS, unsupervised classification was used independently, and in an integrated fashion with the DWT in the extracting of change/no-change information. Unsupervised classification of a given scene is suitable when reliable training data (for supervised classification) are either scarce or expensive, and when relatively little *a priori* information about the data is available. Once a reliable clustering is arrived at, the user can then label the corresponding image segments to obtain a classified image.

Indeed, various unsupervised clustering schemes have been proposed and studied over the years. In particular, classical methods such as *K*-means and ISODATA (Tou and Gonzales 1974), which are based on iterative computations of cluster means, have become standard in the remote sensing community. ISOCLUS is more involved than *K*-means, in the sense that it provides additional heuristic procedures (e.g. cluster merging and splitting) and some interactive features. In this study, the ISOCLUS, which is very similar to ISODATA was implemented. The number of clusters was set to 10 (as the maximum possible number of classes, based on the scene land cover reconnaissance), and termination was applied either after 20 iterations or when a relative change in all of the cluster means did not exceed 1%.

The results for the implemented change detection strategy are presented and described in Section 4.

4. Experimental results

In this section, the results from the study are presented. A brief explanation is provided for the observed results.

4.1 Image differencing results

The results for the multitemporal image differencing for the four tested VIsare presented in Figure 4. The corresponding image statistics in terms of histograms of the SVID images are also presented.

Relating the difference images to the corresponding histograms, and the image statistics presented in Table 1, it is observed that RDVI had the highest variance. RDVI also presented the highest DN ranges (minimum and maximum). This implies that RDVI captured more information in comparison to the other SVI difference images.

From the above SVID results, it is however not straightforward to determine where to place the thresholds for change/no-change information determination. This is when in most studies, trial-and error or parametric Bayesian techniques are used to classify the change/no-change information. It may also be misleading at this stage to conclude that a particular index is the best for this test area, without further statistical and empirical investigations. To further quantify the significance of the results of these indices with regards to the contained change/no-change information, the results were analysed using multiscale wavelet transformation and ISOCLUS, as depicted in the proposed methodology.

4.2 Optimisation of discrete wavelet transform (DWT) results

The five-level 2D-Mexican hat DWT resulted into 18 sub-bands corresponding to the detail images. From the energy computation according to Equation (5), it was observed that as the levels increased, the energy of the sub-bands successively decreased and tended to reach as saturation or convergence as depicted in Figure 5. Levels 3–5 had significantly lower energy than Levels 1 (120 m) and 2 (240 m). This implies that as the resolution gets coarser, significantly lesser information is captured. This may be attributed to the fact that at the coarser spatial resolutions (>240 m) the wavelet transformation process tends to over aggregate the scene landscape characteristics that are also difficult to interpret into classes. Thus for further analysis, Levels 1 and 2 of each of the SVI difference images were selected. Notable is that the vertical sub-band corresponding to the Levels 1 and 2 had consistently lower information. This could relate to the fact that the orientation of most features within the test area is predominantly in the horizontal and diagonal directions.

The explanation for the observations in Figure 5 is attributed to the fact the wavelet high frequency primitives describe image texture. The higher the wavelet level, the larger the textural clumps to be detected. Parts of the rainforest with heterogeneous canopy cover expect to show a lot of texture at around 60 m. This

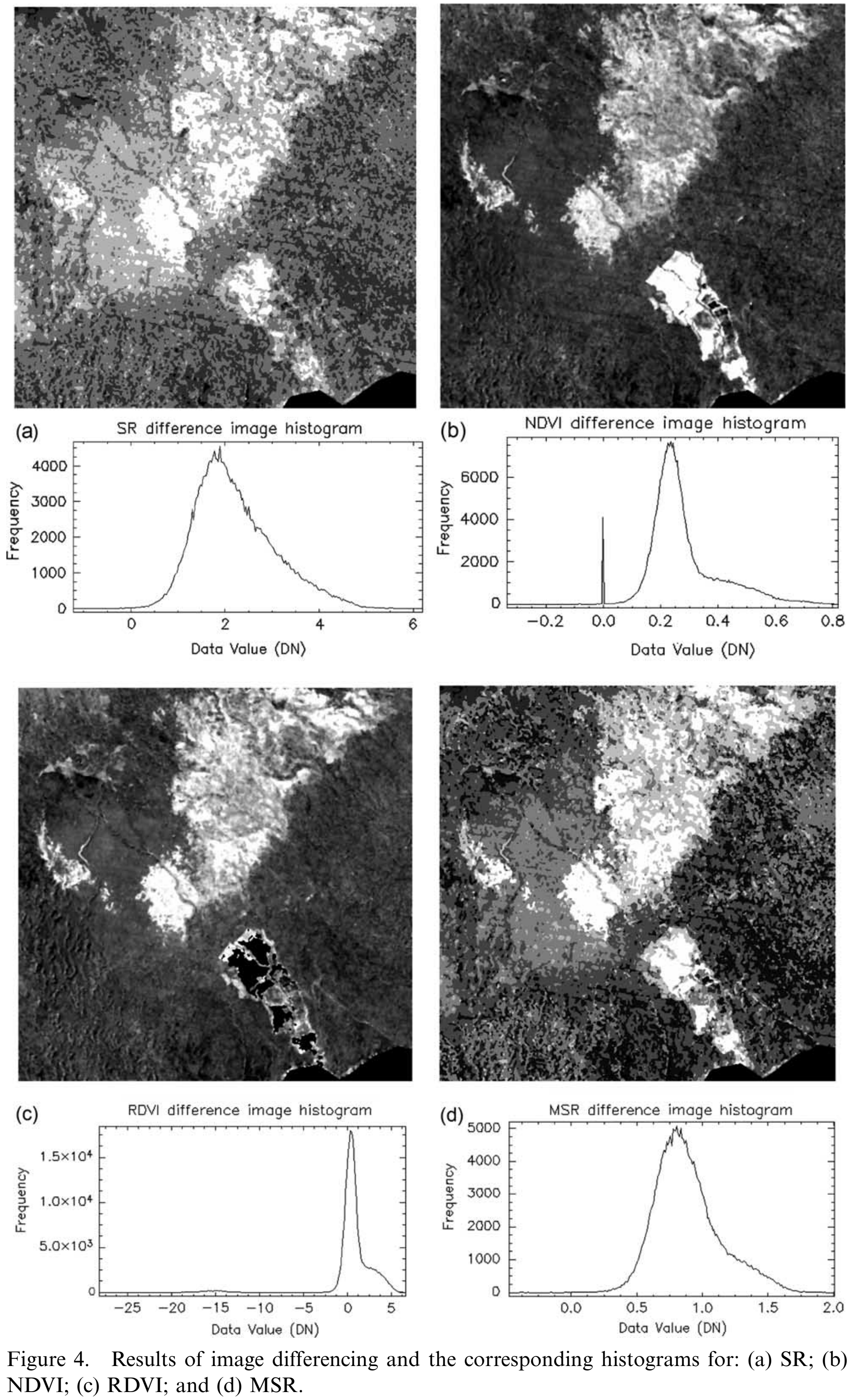

Figure 4. Results of image differencing and the corresponding histograms for: (a) SR; (b) NDVI; (c) RDVI; and (d) MSR.

Table 1. Summary of the SVI difference images statistics.

Difference index	Minimum DN	Maximum DN	Mean	Standard deviation
SR	−1.23	+6.20	2.202	0.871
NDVI	−0.34	+0.82	0.280	0.119
RDVI	−28.22	+6.67	0.788	2.412
MSR	−0.48	+2.02	0.880	0.270

texture will rapidly decrease when pixels of 120 m, and more are used to represent such terrain. This explains the decrease in energy content depicted in Figure 5. High heterogeneity is observed in areas with small-scale farms and illegally logged trees, and thus detectable in the high frequency wavelet primitives of the second level. This

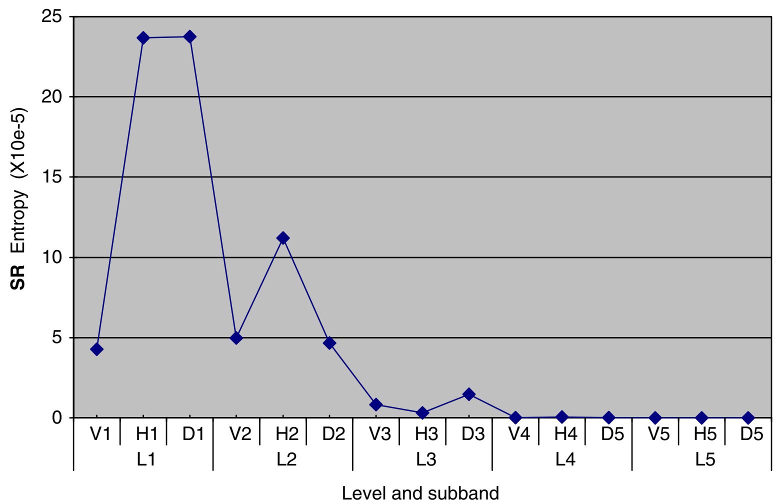

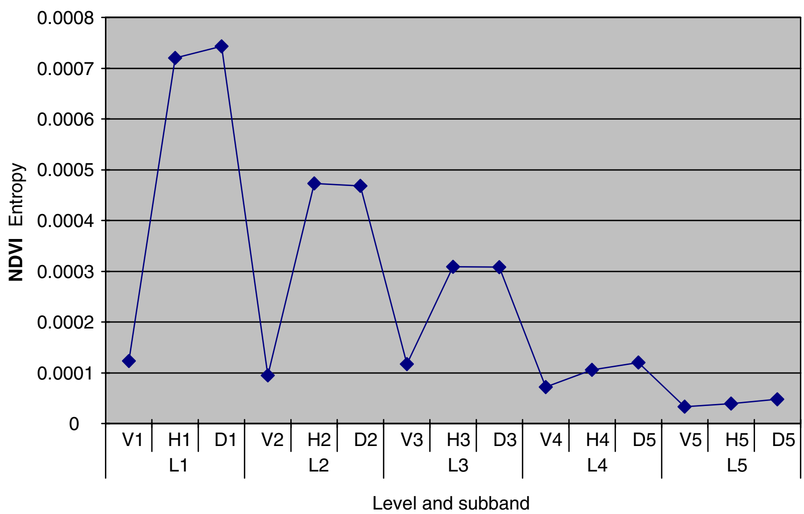

Figure 5. Energy measures for the 15 bands of SR, NDVI, RDVI and MSR, respectively.

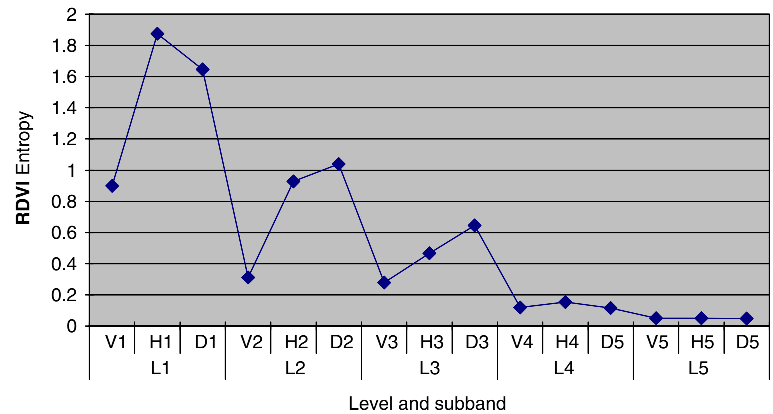

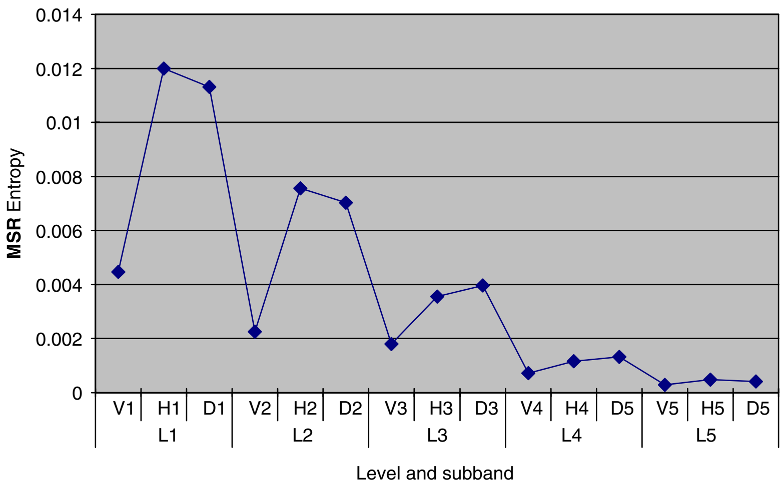

Figure 5 (*Continued*)

explains the need to combine the two DWT levels, in order to capture the textural information captured in the two levels. This observation motivates and justifies the scale-driven fusion of the most informative detail sub-bands.

The next task of isolating the change/no-change information from the optimal RDV–DWT into their respective classes was carried out using ISOCLUS. A comparison of the corresponding sub-bands in RDVI Levels 1 and 2 was carried out. It was found that the following bands/band combinations were the most informative: (i) Level 1 – vertical sub-band; (ii) Levels 1 and 2 – horizontal sub-bands combination; and (iii) Levels 1 and 2 – diagonal sub-bands combination. These selected sub-bands were fused and classified using ISOCLUS.

4.3. Discrete wavelet transform (DWT) results on the Spectral Vegetation Index Differencing (SVID) images

Within the wavelet transform images, the no-change regions are automatically represented by zero-grey level values (dark patches), and the changed regions have varied DN values depending on the ground land cover type. To thematically map and quantify the change classes, the ISOCLUS algorithm is used. This is attributed to the fact that the classes are isolated not only based on the spectral signatures, but also on the basis of frequency patterns. These patterns depend on the directions or orientations inhibited by the specific land cover category. To convert the combined scale levels into ground classes, ground-truth data was used to correlate the DN values/tones recorded in the transformed difference image to the respective change classes.

From the DWT–ISOCLUS approach, the following eight classes were determined: *class 1*: cleared-land/bare-ground; *class 2:* dead bamboo stocks; *class 3:* weathered bamboo, understory and logging; *class 4:* regenerating bamboo and regenerating natural trees within mixed forest; *class 5:* mature tea plantations, farm crops; *class 6:* young tea plantations; *class 7:* tree plantations; and *class 8:* un-changed natural forest cover.

4.3.1 Accuracy assessment of the discrete wavelet transform (DWT) results

The accuracy of the integrated DWT–ISOCLUS results was assessed using reference data in sub-section 2.1. Four performance indices were derived from the confusion error matrix namely: overall accuracy and KAPPA coefficient – for the entire scene; and for the individual classes, the omission and commission errors (or user and producer accuracies) were used.

The overall accuracy and KAPPA coefficient results for the accuracy assessments are presented in Table 2. Table 2 shows that RDVI gave the highest overall accuracy of 91.68% in mapping the change information. This was followed decreasingly by: MSR (82.55%), NDVI (79.73%) and lastly SR (65.34%). The RDVI results point to the theoretical reasoning that the accuracy or performance of the SVI may be related to its variance information (presented in Table 1).

Per-class errors of omission and commission (Tso and Mather 2001) were computed for the eight-classes, with the results presented in Figure 6. The results show that the un-changed class (*class 8*) areas were consistently mapped with the highest accuracy in all the four vegetation indices. The class accuracy results shows that the user's accuracy ranges from 38.6% for *class 6* using NDVI to 98.2% for *class 7* with RDVI class, while the producer's accuracy ranges from 40.6% for *class 3* using SR to 94.3% for *class 4* with RDVI. *Class 3* and *class 6* constantly registered the lowest users' and producers' accuracy in SR and NDVI. The other observed

Table 2. Results of the level of agreement with ground-truth reference data expressed in terms of the overall accuracy percent and KAPPA coefficient.

	Overall accuracy (%)	KAPPA coefficient
SR	65.34	0.528
NDVI	79.73	0.685
RDVI	91.68	0.901
MSR	82.55	0.733

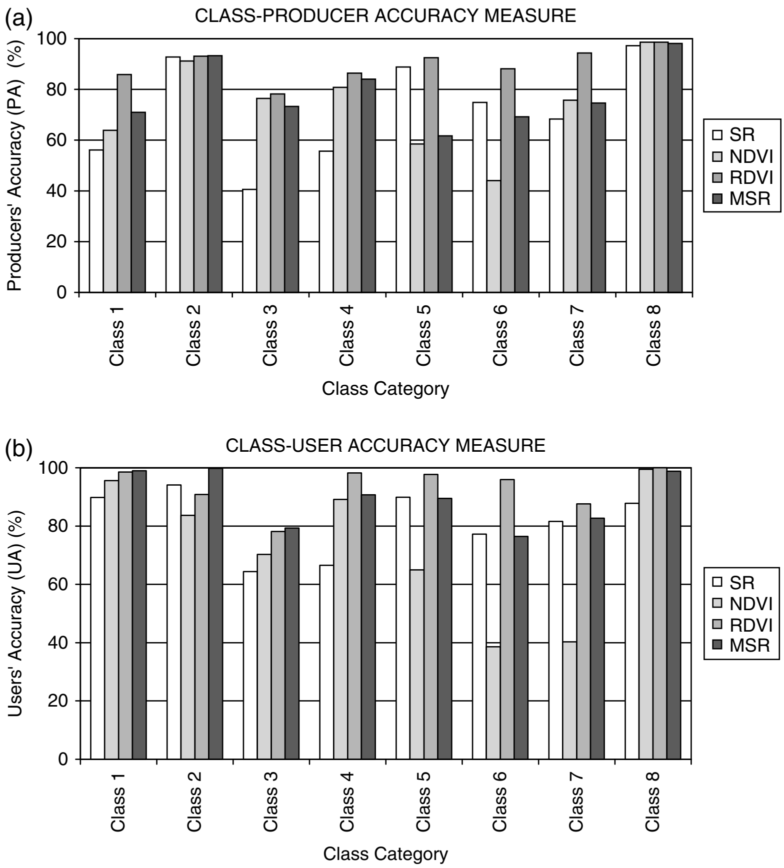

Figure 6. (a) Producers' accuracy results for the eight classes from the four VIs; and (b) Users' accuracy results for the eight classes from the four VIs.

differences were only in the classes that were difficult to discriminate due to their spectral similarity and due to the fact that these classes were mixed within a spatial location e.g. small scale mixed agricultural practices.

From the above accuracy results, RDVI presented the best overall results especially in the spectrally difficult to discern classes like *class 5*, in comparison to the other classes. SR in some cases, performed marginally or far better than NDVI and MSR, e.g. in discerning *class* 2, *class* 5 and *class* 6. The SR class-based performance can be attributed to its higher variance than that of MSR and NDVI (Table 1). Nevertheless, it (SR) had the least overall accuracy and KAPPA coefficient values. *A-posteriori* spectral reflectance curve analysis showed that the selection of the RDVI was accurate, as RDVI presented the best spectral separability between the representative classes. This observation can also be empirically inferred from the RDVI–SVID image in comparison to the other classes, in the representation of the scene features with the different grey-tones. Figure 7 presents the results of the integrated DWT–ISOCLUS strategy.

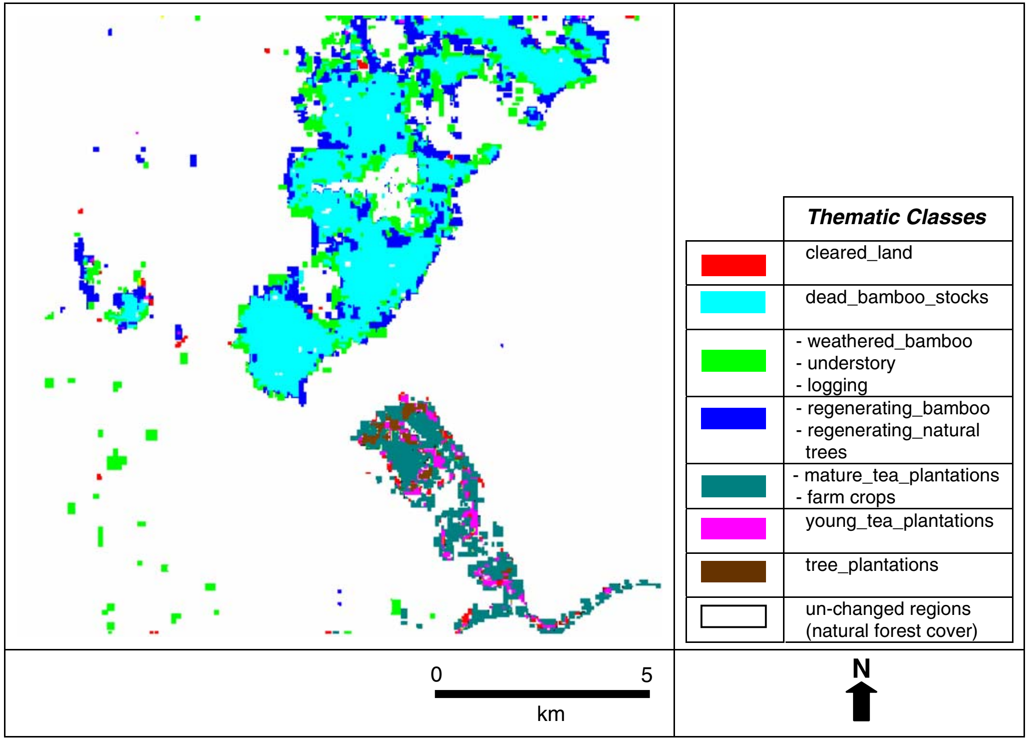

Figure 7. The change/no-change map obtained from the optimal DWT combinations and classified using ISOCLUS clustering technique.

4.4 ISOCLUS-based extraction of change information

From independent ISOCLUS classification on the RDVI, only three classes, apart from the un-changed regions, were uniquely separable: crop plantations, degenerated bamboo areas and dead bamboo stocks (Figure 8). The ISOCLUS approach could not separate between the semi-dead bamboo stocks and tree plantations and other classes, as was the case in the DWT–ISOCLUS. Also some of the crop plantations were classified the same as illegally logged areas.

A comparison of the ISOCLUS approach and the optimal DWT–RDVI showed that the DWT–RDVI performed better, by 42.65%, in isolating the various natural forest changes. This depicts the fact that unsupervised classifiers, especially in spectrally similar areas, may not perform well in capturing such landscape features. This is in part due to their lack in the feature-differentiation based on textural properties.

5. Discussions

Many techniques have been proposed for change detection in both optical and synthetic aperture radar (SAR) remote sensing data. Often, changes are identified by comparing pixel by pixel two images that are acquired on the same geographical area at two different times. The comparison can be carried out according to a difference operator (this is the typical case of multispectral images) or a ratio/log-ratio operator (as usually done in a SAR image), as well as with more complex strategies based on context-sensitive dissimilarity measures that are computed between statistical distributions. The resulting difference/ratio image is then analysed according to either automatic thresholding algorithms, or complex context-sensitive and multi-scale algorithms to generate the final change-detection map. Focusing on thresholding algorithms, which are the most widely used in the applications, the thresholding algorithms derive automatically the change-detection map under the assumption that the prior probability of the class of changed pixels is sufficient to properly model this class with a significant statistical mode in the histogram of the difference/ratio image. However, as the aforementioned kinds of forest changes typically affect local portions of wide areas (e.g. regions or countries), a proper forest change-assessment procedure requires the analysis of wide scenes and, thus, of large-size images. This results in a small value of the prior probability of the class of changed pixels, which may affect the capabilities of the thresholding techniques to detect a proper threshold value if working on the whole image.

In the image-processing literature, local adaptive thresholding techniques have been proposed for characterising the local properties of images. In change-detection problems, these techniques compute a threshold value for each pixel neighbourhood on the basis of local statistics and apply it to either the entire neighbourhood or only the central pixel. As these methods result in many isolated change pixels and holes in the middle of connected change components, post-processing steps are usually adopted for reducing noise in the final change-detection map and making it consistent with the hypothesis that changes are made up of a significant number of connected pixels. Alternative approaches, which are mainly proposed for threshold-based classification of large-size images, perform an independent analysis of

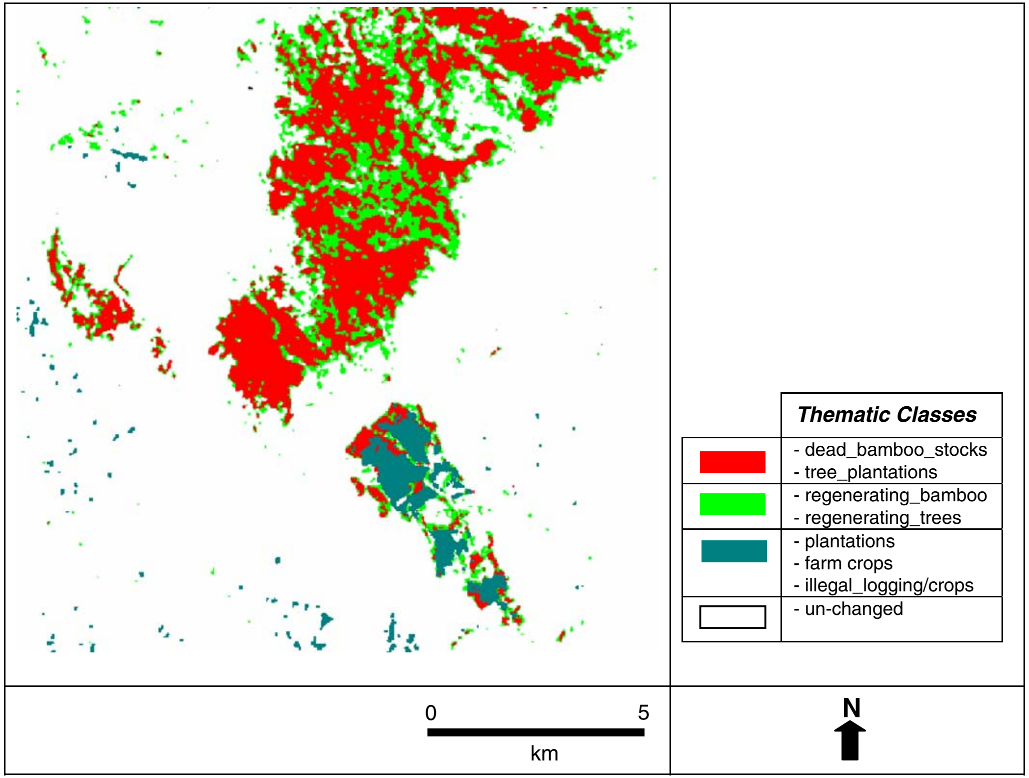

Figure 8. ISOCLUS classification results depicting the change/no-change map from the RDVI.

multitemporal image data that results in different threshold values for each considered region.

The experimental results in this study, based on the proposed DWT–ISOCLUS approach, showed that all the compared indices performed better than 60%. The significant difference among the SVIs could be from their independent inabilities to isolate specific land cover that are spectrally very similar: for example tea plantations from tree plantations, cash crops from subsistence crops (i.e. tea from maize), and young from mature tree plantations. These though are only characteristic to this case study. Within less spectrally homogeneous areas, the proposed approach may perform much better, but care must be taken that the optimal results may not necessarily be from the RDVI.

In practise, most of the change-detection methods usually involve the utility of more spectral channels with the notion that it is more suitable to search the change information within a wider spectral spectrum. Though this is a logical argument, this study demonstrated that for forest change detection, the SR-based RDVI yielded promising results. The impressive result from RDVI implies a minimised signal-to-noise ratio by the index, and is significant because linear relationships with ground biophysical parameters help simplify remote sensing data analysis and improve the accuracy in retrieving these surface parameters (Roujean and Breon 1995).

It can be argued that the reason why the RDVI performed much better in this application is because classes of interest are discriminated well in the low to medium vegetation cover range. For other applications where the landscape is predominately natural forest and soil, i.e. no human activities, it is suggested to use the modified soil-adjusted vegetation index (MSVI2ˆ0.5) to capture the two main land cover information.

It should be noted that forests can be distinguished from many other land cover types by high texture in the red band (*red-edge*) often referred to as high standard deviation or heterogeneity, calculated with a moving window over the red band covering forests. However due to the spatial, textural and spectral heterogeneity of forest landscapes, not all the desirable information can be captured from the red band alone. Thus VIs should be relied upon to capture the spectral and textural information in other significant bands. The fundamental question that arises is how to capture these spectral and textural feature primitives from the indices.

The proposed DWT–ISOCLUS approach was able to isolate change information of different categories. Theoretically, local-region-based change detection is used with informative multiscale approach to improve on the discriminability of the changed/un-changed classes, and to analyse the changes at different scales simultaneously (by scale-driven fusion). This is important in detecting the complex-large landscape changes.

The independent ISOCLUS, in comparison to the optimal DWT–ISOCLUS approach gave an accuracy of only 49.03%. Probably the main reason for the poor performance of the ISOCLUS is the fact the partial forest disturbances are more difficult to detect, and requires additional primitives such as textural information.

Focusing on the DWT–ISOCLUS, the number of the scales was varied in the range [1, 5] (Figure 9). When just one scale is used ($s = 1$), the method degenerates 84.07%. A higher detection accuracy is obtained, as determined before, when using the first two scales (i.e. $s = 1$). The overall accuracy results deteriorate as the number of scales increase from ($s = 3$, 4 and 5), as shown in Figure 9. When ($s = 5$), the results

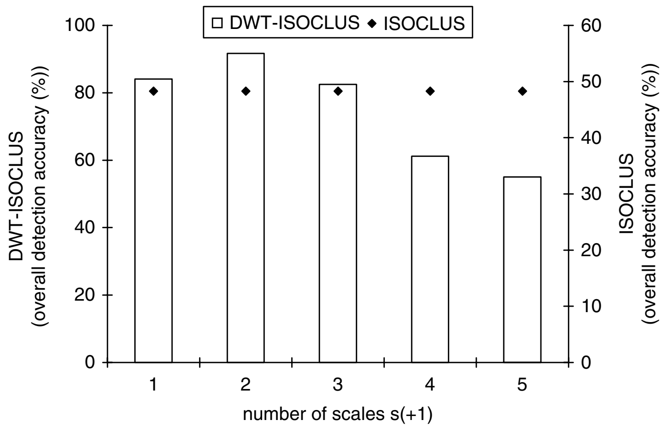

Figure 9. Behaviour of the detection accuracy as a function of the number of considered scales for the DWT–ISOCLUS, against the 48.3% ISOCLUS accuracy.

near that of the standard ISOCLUS classification results. These results confirm the importance of the scale-driven information optimisation in the proposed method, and suggest sensitivity to the number and location of the scales.

6. Summary and conclusions

This study presented comparative-unsupervised approach for digital change detection by exploring the potential of SR-based multitemporal SVI differencing and transformation for change type determination within forest systems. The SVI difference images were compared using DWT and ISOCLUS classification for isolation of change/no-change information. RDVI gave the best results as depicted by highest KAPPA coefficient and overall accuracy statistics in comparison with SR, NDVI and MSR indices. With regards to change type isolation, it was found that DWT combined with ISOCLUS performed much better than the independent ISOCLUS on the optimal (RDVI) difference image.

The experimental results reported in this paper confirm the effectiveness of the presented techniques. Such effectiveness depends mainly on the powerful ability provided by local-region-based change detection and multiscale fusion. Thanks to this ability, the proposed approach turns out to be superior to the traditional method. Despite the promising preliminary results, the accuracy needs to be further improved in future developments especially in the changed region borders.

The results show that a hierarchal-statistical selection and integrated wavelet analysis represents a powerful set of image processing capabilities that have considerable potential to quantify ecologically relevant patterns at multiple scales. The presented technique shows both high sensitivity to geometrical details and a high robustness to noisy components in homogeneous areas and heterogeneous land cover. The approach has considerable potential for the long-term monitoring of vegetation change from multisensor remotely sensed imagery.

The methodology suggested in this study presents a cost-effective and practical method to detect land-cover changes to support decision making for updating forest databases. Further comparisons of other wavelet transforms will be tested to infer their significance in related tasks of larger extents. Also for further research, the Markov Random Field (MRF) multiscale fusion and classification-based system will be tested against the current approach, as a means of integrating the DWT features and the spatial contextual information.

Finally, the relevance of the current research to Digital Earth lies in the benefit in the digital geo-data acquisition, data mining and representation of one of the key components of the earth i.e. forest dynamics or space-time digital representation and analysis. Such data goes a long way in informing the public sector, private sector and decision makers in the collective conservation and management of the earth, more so as the world experiences a raise in carbon emissions and the consequences related thereto, such as drought and global warming. It is envisaged that the model presented in this paper can be extended to the national, trans-boundary and global visualisation of the forest dynamics, much more accurately, via more intelligent digital image descriptors.

Acknowledgements

The authors would like to acknowledge the Research Grant from the Japanese Ministry of Science and Education (MEXT). The authors appreciate the comments from the anonymous reviewers. Their suggestions have significantly improved the paper.

Notes on contributors

Dr. Yashon O. Ouma received BSc(Eng) in Surveying and Photogrammetry from the University of Nairobi (Kenya) in 1994; MSc(Eng) in Geomatics from the University of Cape Town (South Africa) in 1999, and Dr(Eng) from the Graduate School of Science and Technology and CEReS from Chiba University (2006) in Japan. Dr. Ouma is a Senior Lecturer in the Department of Civil and Structural Engineering of the School of Engineering, Moi University in Kenya. Since 2008, he has been the Editor-in-Chief of the African Journal of Technology, and is a Member of the UNSAC. His main interests are social-economic and spatial data analysis, regional analysis, GIS implementation, and satellite image processing for analysis of the urban and natural environment, with special attention to image textural and image multiscale segmentation and classification techniques and new structure-based multi-scale image fusion approaches.

Prof. Dr. Ryutaro Tateishi received his Doctor of Engineering degree from the University of Tokyo in 1982. Prof. Tateishi is a Full Professor at the Center for Environmental Remote Sensing (CEReS), Chiba University. His research activities are in the field of land remote sensing, currently focusing on global land cover mapping and monitoring. He served the International Society for Photogrammetry and Remote Sensing (ISPRS) as a Commission Secretary and Working Group Chairman from 1988 to 2004. He has remained Chairman of International Steering Committee for Global Mapping (ISCGM) WG 4 on raster data development since 2002. He is currently a President of Remote Sensing Society of Japan.

References

Bannari, A., *et al.*, 1995. A review of vegetation indices. *Remote Sensing Reviews*, 13, 95–120.

Carvalho, L.M.T., *et al.*, 2001. Digital change detection with the aid of multi-resolution wavelet analysis. *International Journal of Remote Sensing*, 22 (18), 3871–3876.

Chen, J.M., 1996. Evaluation of vegetation indices and a modified simple ratio for boreal application. *Canadian Journal of Remote Sensing*, 22 (3), 229–242.

Clark, D.K., *et al.*, 1997. Validation of atmospheric correction over oceans. *Journal of Geophysical Research*, 102 (D14), 209–217.

Clark, R.N., *et al.*, 2002. Surface reflectance calibration of terrestrial imaging spectroscopy data: a tutorial using AVIRIS. *In*: R.O. Green, ed. *Proceedings of the 10th Airborne Earth Science Workshop*, 10 October 1998, JPL Publication 02-1, 2002. Pasadena, CA: Jet Propulsion laboratory, 21–30.

Coppin, P.R. and Bauer, M.E., 1996. Digital change detection in forest ecosystems with remotely sensed imagery. *Remote Sensing Reviews*, 13, 207–234.

Daubechies, I., 1991. *Ten lessons on wavelets.* CMBS-NSF Series Applications in Mathematics, SIAM.

FAO, 2006. *Global forest resources assessment 2005*. Food and Agriculture Organization of the United Nations (FAO), Forestry Report Paper No. 147, Rome.

Fung, T. and Siu, W., 2000. Environmental quality and its changes, an analysis using NDVI. *International Journal of Remote Sensing*, 21 (5), 1011–1024.

Goetz, A.F.H., *et al.*, 1998. Using ground spectral irradiance for model correction of AVIRIS data. *AVIRIS 1998 Proceedings.* Pasadena, CA: JPL, 10pp.

Kalácska, M., *et al.*, 2004. Leaf area index measurements in a tropical moist forest: a case study from Costa Rica. *Remote Sensing of Environment*, 91 (2), 134–152.

Karpouzli, E. and Malthus, T., 2003. The empirical line method for the atmospheric correction of IKONOS imagery. *International Journal of Remote Sensing*, 24 (5), 1143–1150.

Lyon, J.G., *et al.*, 1998. A change detection experiment using vegetation indices. *Photogrammetric Engineering and Remote Sensing*, 64 (2), 143–150.

Mallat, S., 1989. A theory for multiresolution signal decomposition. *IEEE Pattern Analysis and Machine Intelligence (PAMI)*, 31 July–4 August 2006, Denver, CO, 11 (7), 17–34.

Memarsadeghi, N., Le Moigne, J., and Mount, D., 2006. Image fusion using cokriging. *IEEE-IGARSS 2006*, 2518–2521.

North, P.R.J., 2002. Estimation of fAPAR, LAI, and vegetation fractional cover from ATSR-2 imagery. *Remote Sensing of Environment*, 80 (1), 114–121.

Roujean, J-L. and Breon, F.M., 1995. Estimating PAR absorbed by vegetation from bidirectional reflectance measurements. *Remote Sensing of Environment*, 51, 375–384.

PCI, 1999. *EASY/PACE software package, version 6.3*. Richmond Hill, ON: PCI.

Tou, J.T. and Gonzales, R.C., 1974. *Pattern recognition principles.* Reading, MA: Addison Wesley.

Tso, B. and Mather, P.M., 2001. *Classification methods for remotely sensed data*. London: Taylor and Francis.

Young, S.S. and Wang, C.Y., 2001. Land-cover change analysis of China using global-scale Pathfinder AVHRR Landcover (PAL) data, 1982–92. *International Journal of Remote Sensing*, 22 (8), 1457–1477.

Yu, J. and Ekström, M., 2003. Multispectral image classification using wavelets: a simulation study. *Pattern Recognition*, 36 (4), 889–898.